

Inelastic Scattering, Emergent Interactions of Solitons in the Zakharov-Kuznetsov Equation through Conservative and non-Conservative Physics-Informed Neural Networks

A. Nakamura,^{1,*} K. Obuse,^{2,†} N. Sawado,^{3,‡} K. Shimasaki,^{3,§}

Y. Shimazaki,^{3,¶} Y. Suzuki,^{3,**} and K. Toda^{4,5,††}

¹*Department of Physics, School of Science,
Kitasato University, Sagami-hara, Kanagawa 252-0373, Japan*

²*Graduate School of Environmental and Life Science,
Okayama University, Okayama 700-8530, Japan*

³*Department of Physics and Astronomy, Tokyo University of Science, Noda, Chiba 278-8510, Japan*

⁴*Department of Mathematical Physics, Toyama Prefectural University, Imizu, Toyama 939-0398, Japan*

⁵*Research and Education Center for Natural Sciences, Keio University,
Hiyoshi 4-1-1, Yokohama, Kanagawa 223-8521, Japan*

Physics-Informed Neural Networks (PINNs) are used to study collision process of soliton solutions in the 2+1 dimensional Zakharov-Kuznetsov equation. The Zakharov-Kuznetsov equation originally was the model in three dimensions of plasma with a uniform magnetic field and it is a direct extension of the KdV equation into higher dimensions and is a typical quasi-integrable system. PINNs successfully solve the equations in the forward process and the solutions are obtained using the mesh-free approach and automatic differentiation while accounting for conservation laws. In the inverse process, the proper form of the equation can be successfully derived from a given training data. On the other hand, the situation becomes weird in the collision process. The result in the forward analysis no longer possesses the conservation laws, which is ought to be referred to as a dynamically incompatible field configuration (DIFC) instead of the solutions of the system. Conservative PINNs are thus introduced and we succeed to obtain the solutions that satisfy the conservation laws. The inverse analysis suggests a different equation where the coefficients exhibit the significant changes, which implies an emergent temporal interaction. With these modulated coefficients, we recalculate the equation and confirm that the conservation law has unquestionably improved.

* nakamura@sci.kitasato-u.ac.jp

† obuse@okayama-u.ac.jp

‡ sawadoph@rs.tus.ac.jp

§ shimasakit@gmail.com

¶ shimazakit@gmail.com

** ytszkyuta@gmail.com

†† kouichi@yukawa.kyoto-u.ac.jp

I. INTRODUCTION

In recent years, there has been a lot of interest in applying deep learning methods—specifically, deep neural networks—to nonlinear partial differential equations (PDEs). Numerous complex scientific problems, including those in fluid and solid mechanics [1–10], cyber-physical systems [11], biological systems [12–15], can efficiently be resolved by the Physics-Informed Neural Networks (PINNs) [16–18]. One remarkable feature of PINNs is that, in addition to solving PDEs easily (the forward analysis), they may also provide us a precise estimate of the equation based on the governing data of the physical issues of our concern (the inverse analysis). PINNs have significantly higher extrapolation power compared to other conventional deep-learning techniques, making them appropriate for analyses involving limited learning data [19–21].

Notably, PINNs are completely different scheme from the traditional, standard numerical algorithm as claimed in Refs.[22–26]. Many numerical studies have been conducted on the finite difference and finite element methods, where the governing PDEs are ultimately discretized over the computational domain. On the other hand, the unique, outstanding feature of PINNs is their mesh-free methodology, as automatic differentiation approximates the differential operators in the governing PDEs. PINNs’ grid independence is undoubtedly efficient particularly for solving high-dimensional problems and also inverse analysis. The inverse PINNs analysis may give us the ability to verify the validity of a solution that is derived using the conventional finite difference method. It is our main concern in the paper. An additional benefit of utilizing PINNs is their ability to integrate conservation laws of a system into analysis by incorporating the condition into the loss function. The method called conserved-Physics-Informed Neural Networks (cPINNs) gains the accuracy of the analysis [22, 27–30]. Ref.[30] employs the standard project method from geometric numerical integration into PINNs and says an exact or a *hard-conservative* method. As far as we know, no similar technique was known with nonlinear-wave analysis. In Ref.[31], We presented a bit sophisticated cPINN technique (but not the *hard* method), where we included a weight function $C(\mathcal{E})$ that allows us to regulate the loss function’s convergence property.

There are numerous studies of PINNs for the integrable PDEs, such as the Bergers eq. [16–18, 22, 27], the KdV eq. and the modified KdV eq. [22, 28, 32–35], the nonlinear Schrödinger eq. [36, 37], a coupled Schrödinger-KdV eq. [38] and many other variations. In 2+1 dimensions, the KP eq.and the spin-nonlinear Schrödinger eq. were studied via PINNs [39–41], respectively. There are analyses for quasi-integrable deformations of the KdV eq. [42, 43]. We studied two quasi-integrable equations in 2+1-dimensions and thoroughly discussed how the inverse PINNs identified

them [31].

In the present paper, we analyze property of the several configurations of the Zakharov-Kuznetsov equation using the PINNs analysis. The ZK eq. [44, 45] is a direct extension of the KdV equation into higher dimensions. At the moment the researches [45–47] have focused on the two-dimensional version of the model. The equation possesses stable isolated vortex-type soliton solutions which enjoy normal solitonic properties, i.e., they move a constant speed without dissipation and possess a number of conservation quantities. As a result, they have a certain longevity about the standard computational time-scale. Therefore, they may be a possible candidate of the vortex in the fluid dynamics, e.g., the Great Red Spot (GRS) of Jupiter [48]. On the other hand, inelastic properties emerge when the heights of solitons significantly differ, in a collision process the taller soliton gains more height while the shorter one tends to wane with the radiation [45]. These odd inelastic solitons are frequently found in a number of quasi-integrable systems [49–52], which are caused by insufficient conservation quantities. Many of the integrable and the quasi-integrable equations have origin with fluid mechanics or plasma physics. Although they are almost on same footing physically, there are few studies that explore the mathematical property as the initial value problem of the quasi-integrable equations. The rare exception was for the 1+1 regularized long-wave equation [53]. A crucial question is whether linear superposed configurations in these quasi-integrable equations could be solutions, which has been overlooked for many years. In this paper, we will address this issue. In order to distinguish these anomalous objects from the known, well-behaved soliton solution, we introduce the concept: dynamically incompatible field configuration (DIFC). Therefore, the main objective of the present paper is to apply forward/inverse PINNs/cPINNs to some DIFC, namely in the collision process of the 2+1 Zakharov-Kuznetsov (ZK) equation.

The paper is organized as follows. In Section II, we give a brief introduction of the Zakharov-Kuznetsov equation. We present an overview of Physics Informed Neural Networks and also the basic formalism of our cPINNs in this section. In Section III, we give our numerical results including discussion for the coefficient modulations in the inverse PINNs. This section contains discussions regarding the coincidence or disagreement between the forward and inverse analyses. The conclusions and remarks are presented in the last section.

II. ZAKHAROV-KUZNETSOV EQUATION

Zakharov-Kuznetsov equation originally was the model in three dimensions of plasma with a uniform magnetic field [44]. It simply be regarded as a direct extension of the KdV equation into higher dimensions and is a typical quasi-integrable system. Though the term “quasi-integrability” is frequently employed in literature, mathematically it is still a bit obscure. One simple definition of a quasi-integrable system is an equation that has only a finite number of exact conservation quantities. We investigate the Zakharov-Kuznetsov equation from this simple perspective, whose solutions resemble solitons in the integrable system, having just four conservation quantities. At the moment most of the researches [45–47] have focused on the two-dimensional version of the model. One prominent aspect of the solution in the equation lies in some irregular inelastic features of the collision process. When the heights of solitons coincide, the collision looks similar with the integrable cases. On the other hand, when they are significantly different, during a collision process the taller soliton gains more height while the shorter one tends to wane with the radiation [45]. Further, when we consider a case of offset scattering, the shorter soliton tends to disappear after the impact of the collision.

The Zakharov-Kuznetsov (ZK) equation

$$\frac{\partial u}{\partial t} + 2u \frac{\partial u}{\partial x} + \frac{\partial}{\partial x} (\nabla^2 u) = 0 \quad (1)$$

where the Laplacian specifies $\nabla^2 = \partial_x^2 + \partial_y^2$. Eq.(1) possesses meta-stable isolated vortex-type solutions which enjoy the solitonic properties. The equation possesses the solutions propagating in a specific direction with uniform speeds. Here we set the direction in the positive x orientation with the velocity c , namely assuming $u = U(\tilde{x} := x - ct, y)$. Plugging it into (1), we obtain

$$\nabla^2 U = cU - U^2, \quad (2)$$

where $\nabla^2 = \partial_{\tilde{x}}^2 + \partial_y^2$. A steady progressive exact wave solution is of the form

$$U_{1d} = \frac{3c}{2} \operatorname{sech}^2 \left[\frac{\sqrt{c}}{2} (\tilde{x} \cos \theta + y \sin \theta) \right], \quad (3)$$

where the θ is a given inclined angle of the solution. It indicates that this solution is just a trivial embedding of the KdV soliton into two spatial dimensions. Eq.(2) possesses another solution keeping circular symmetry other than (3). In order to find it, we introduce cylindrical coordinates and rewrite the equation as

$$\frac{1}{r} \frac{d}{dr} \left(r \frac{dU(r)}{dr} \right) = cU(r) - U(r)^2, \quad (4)$$

where $r := \sqrt{\tilde{x}^2 + y^2}$. We are able to find the solutions with the boundary condition $U \rightarrow 0$ as $r \rightarrow \infty$ numerically and the solutions form one parameter family of c such as $U(r) := cF(\sqrt{cr})$.

The solutions of (1) exhibit solitonic behavior; however, they are not like known integrable solitons, as those of the KdV equation, in that the stability of the solutions may be supported by the infinite number of conserved quantities in the equation. Eq.(1) admits only the four integrals of motion [54], which are

$$I_1 := \int i_1(y)dy = \int u dx dy, \quad i_1(y) := \int u dx, \quad (5)$$

$$I_2 := \int \frac{1}{2} u^2 dx dy, \quad (6)$$

$$I_3 := \int \left[\frac{1}{2} (\nabla u)^2 - \frac{1}{3} u^3 \right] dx dy, \quad (7)$$

$$I_4 := \int \mathbf{r} u dx dy - t \mathbf{e}_x \int u^2 dx dy, \quad (8)$$

where \mathbf{r} and \mathbf{e}_x are the two-dimensional position vector and the unit vector in the x -direction. Here I_1 is interpreted as the ‘‘mass’’ of the solution, and $i_1(y)$ itself is conserved similarly to the KdV equation, respectively. Also, I_2, I_3, I_4 mean the momentum, the energy, and the laws for the center of mass, respectively. We, therefore, conclude that the ZK equation is not an integrable system in the manner of ordinary soliton equations.

A. Methods: algorithms of PINNs and cPINNs

The method consists of two parts of the networks. The first segment is the well-known neural networks part, which is constructed with 4 hidden layers and 20 nodes for which each layer to get the output u from the inputs, time-spatial coordinates (t, x, y) . However, the output of this network has no physical meaning. In the second segment, the output derivatives and a loss function for network optimization are estimated (see See 3.2 and 3.3 in detail).

The PINNs can be applied to both forward and inverse problems. One can find solutions to a governing equation through the forward analysis without usage of large computational resources or sophisticated numerical algorithms. Let us consider the ZK equation of the form

$$\mathcal{F} := u_t + \mathcal{N}(u, u_x, u_{xxx}, u_{xyy}) = 0, \quad \mathcal{N}(u, u_x, u_{xxx}, u_{xyy}) := 2uu_x + (\nabla^2 u)_x, \quad (9)$$

We focus on the soliton solutions moving to the positive x direction. We define the rectangular

mesh space

$$\begin{aligned} x &\in [-L_x, L_x], N_x \text{th grid points}; & y &\in [-L_y, L_y], N_y \text{th grid points}, \\ t &\in [T_0, T_1] \end{aligned} \quad (10)$$

For optimization of the networks, the mean-squared error function: MSE is implemented as the loss function to measure the discrepancy between the predicted values and the correct ones, which can be chosen such that

$$MSE := MSE_{\text{init}} + MSE_{\text{eq}} + MSE_{\text{bc}} \quad (11)$$

$$MSE_{\text{init}} := \frac{1}{N_u} \sum_{i=1}^{N_u} |u_{\text{pred}}^0(x^i, y^i, 0) - u_{\text{correct}}^0(x^i, y^i, 0)|^2 \quad (12)$$

$$MSE_{\text{eq}} := \frac{1}{N_F} \sum_{i=1}^{N_F} |\mathcal{F}(x^i, y^i, t^i)|^2 \quad (13)$$

where u_{pred}^0 is the predicted initial profile and u_{correct}^0 is the correct initial profile and $\{x^i, y^i, 0\}_{i=1}^{N_u}$ is the N_u th set of random residual points and $\{x^i, y^i, t^i\}_{i=1}^{N_F}$ is the N_F th random points for the PINNs $\mathcal{F}(x, y, t)$. Finally, MSE_{bc} represents mean squared error caused by the boundary conditions with the N_b th random points. Here, the doubly periodic boundary conditions are employed as

$$\begin{aligned} MSE_{\text{bc}} := \frac{1}{N_b} &\left[\sum_{i=1}^{N_{b,x}} |u_{\text{pred}}(x^i, L_y, t^i) - u_{\text{pred}}(x^i, -L_y, t^i)|^2 \right. \\ &\left. + \sum_{j=1}^{N_{b,y}} |u_{\text{pred}}(L_x, y^j, t^j) - u_{\text{pred}}(-L_x, y^j, t^j)|^2 \right]. \end{aligned} \quad (14)$$

where $N_b \equiv N_{b,x} + N_{b,y}$.

Taking into account the conservation law I_i , ($i = 1, \dots, 4$) (5)-(8), i.e.,cPINNs, we add

$$MSE_C := C(\mathcal{E}) \frac{1}{N_p} \sum_{i=1}^4 \sum_{a=1}^{N_p} |I_i^{\text{pred,(a)}} - I_i^{\text{correct,(a)}}|^2 \quad (15)$$

to MSE (11). The weight function $C(\mathcal{E})$ is the key component of this method, and it is evaluated using the conventional MSE: $\mathcal{E} \equiv MSE_B$

$$C(\mathcal{E}) = \begin{cases} \exp(-\gamma \mathcal{E}_{\text{crit}}) & \mathcal{E} > \mathcal{E}_{\text{crit}} \\ \exp(-\gamma \mathcal{E}) & \mathcal{E} \leq \mathcal{E}_{\text{crit}}. \end{cases} \quad (16)$$

It describes the schedule of the network optimization of the simulation. At early stages, the conventional MSE, \mathcal{E} is the main concern. The weight function starts to rely on the value of \mathcal{E} at a specific critical point $\mathcal{E} \sim \mathcal{E}_{\text{crit}}$. The optimization eventually takes precedence for the MSE_C . Here

we introduce two parameters $\gamma, \mathcal{E}_{\text{crit}}$ which define a rate of change of the weight and the following values are selected heuristically for the present study

$$\gamma = 3000, \quad \mathcal{E}_{\text{crit}} = 5.0 \times 10^{-3}.$$

We establish the number N_p th reference time, when the numerical integration by the conventional Simpson method is carried out, for the estimation of the conserved quantities. Since the effect is most noticeable one, we solely employ the second conservation law I_2 in the analysis of the present paper.

Another, more prominent application of PINNs is that the generation of the PDE from given data, known as inverse analysis. Now, we introduce a slightly modified PINNs

$$\tilde{\mathcal{F}} := u_t + \tilde{\mathcal{N}}(u, u_x, u_{xxx}, u_{xyy}, \boldsymbol{\lambda}) = 0, \quad (17)$$

where the unknown parameters $\boldsymbol{\lambda}$ is implemented in the equations. For the inverse analysis, we employ the other MSE as

$$MSE_{\text{inv}} := \frac{1}{N_u} \sum_{i=1}^{N_u} |u_{\text{pred}}(x^i, y^i, t^i) - u_{\text{correct}}(x^i, y^i, t^i)|^2 + \frac{1}{N_F} \sum_{i=1}^{N_F} |\tilde{\mathcal{F}}(x^i, y^i, t^i)|^2, \quad (18)$$

where u_{pred} is the predicted profile and u_{correct} is the correct profile including the boundary data. Varying the parameters of the Neural Networks $(w_{lk}^{(j)}, b_k^{(j)})$ and also the parameters $\boldsymbol{\lambda}$, the networks are properly optimized. As a result, we obtain the proper $\boldsymbol{\lambda}$ and then the idealized equations for corresponding training data. For the cPINNs inverse analysis, we add the (15) into (18). PINNs is tuned by optimizing the MSEs. We employ the optimizer L-BFGS [55]. The convergence is attained when the *MSE* gradient's norm is less than the machine epsilon

$$|\nabla MSE| < \varepsilon, \quad \varepsilon = 2.220 \times 10^{-16}. \quad (19)$$

The analysis is further improved in order to address the long-term simulation demand. In general, PINNs need a lot of training data to handle long-term behavior phenomena, but they also require a significant amount of processing resources. A study of the splitting of the integration intervals is the basis for some of the attempts to increase the training time interval [56, 57]. After many time steps, the findings of PINNs frequently converge to a trivial solution. In this paper, we also employ a multi-time step algorithm for the problem, but we aim to focus on events that may occur during a short time window. We divide total time T into the n -segment

$$t_s \in [T_0 + (s-1)\Delta t, T_0 + s\Delta t], \quad s = 1, \dots, n; \quad \Delta t := \frac{T_1 - T_0}{n}. \quad (20)$$

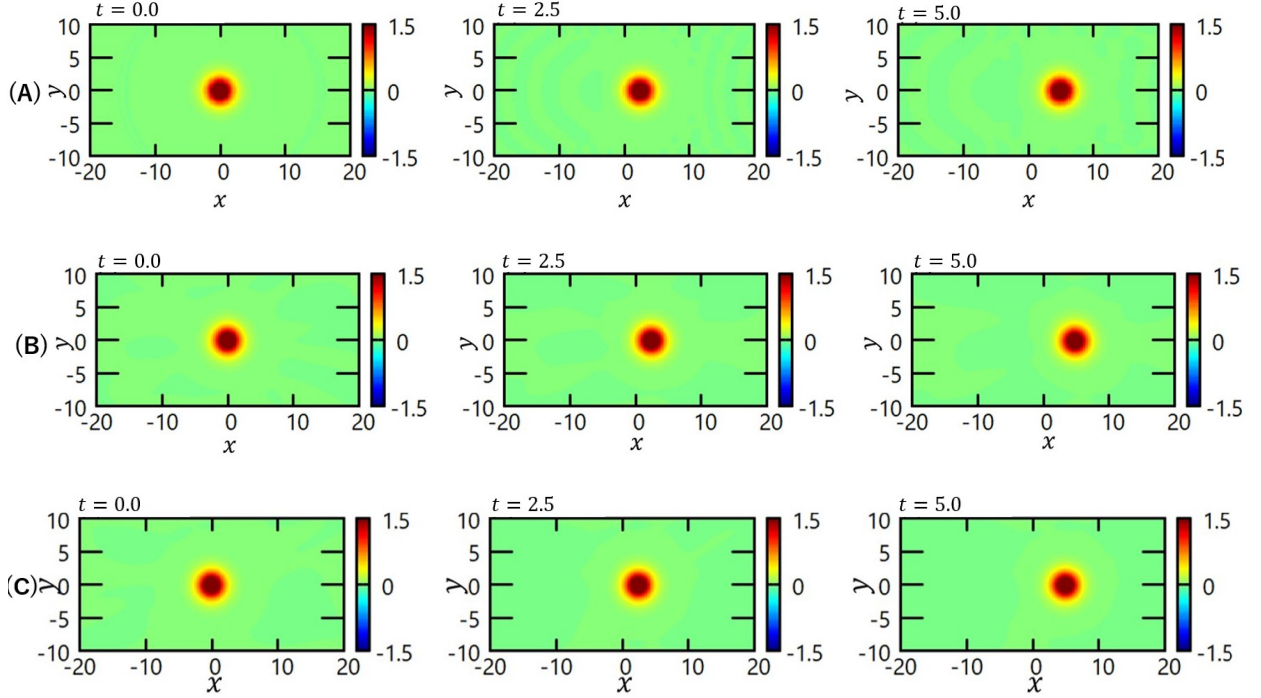


FIG. 1. The solutions of (A) the exact numerical Runge-Kutta method, (B) the PINNs, and (C) the cPINNs for the time $t = 0.0, 2.5, 5.0$.

We begin the PINNs or cPINNs with the first segment $s = 1$ with the initial condition $\{u(x^i, y^i, t = T_0)\}$. Once we obtain the solution $\{u(x^i, y^i, t_{s=1}^i)\}$, the PINNs/cPINNs for the next segment $s = 2$ can be performed with the initial profile $u(x^i, y^i, \Delta t)$. We repeat the procedure until we reach to $s = n$. We perform our analysis for each segment with

$$N_u = 20000, \quad N_F = 50000, \quad N_b = 5000, \quad N_p = 11. \quad (21)$$

We will see in the next section that the inverse analysis results in fluctuations of the equation's coefficients. For our inverse analysis, we thus utilize I_2 for (15) since it is invariant in the presence of such changes.

III. THE NUMERICAL RESULTS

We shall compare the several results of the 1-soliton and 2-soliton configurations in PINNs or cPINNs and the standard Runge-Kutta method. For the inverse analysis, we especially focus on data of the short period segments, allowing us to estimate changes of the coefficients of the equation, which is our current area of interest.

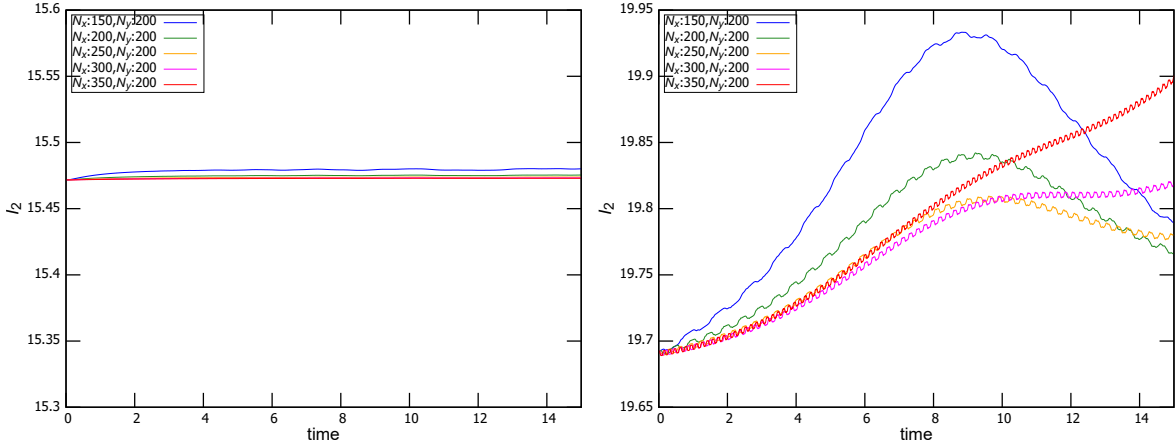


FIG. 2. The conserved quantity I_2 (6) of the 1-soliton (*left*) and the 2-soliton solutions (*right*). The evolution equation is solved by the Runge-Kutta method.

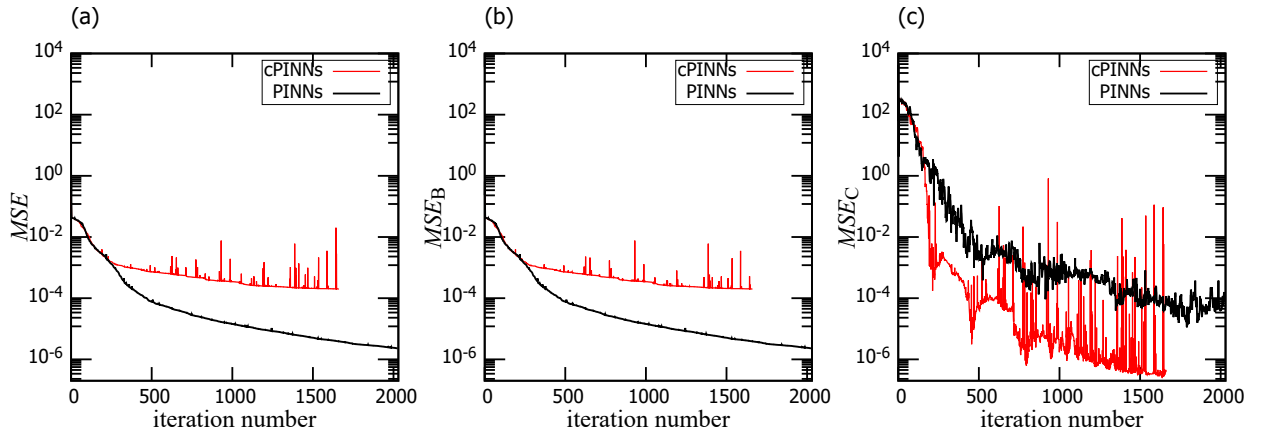


FIG. 3. The MSEs of the PINNs and cPINNs solutions with $c = 1.0, 0.25$. (a) the total MSE , (b) the MSE_B , (c) the MSE_C .

A. The forward analysis

In Fig.1, we plot results of the 1-soliton solutions of the time $t = 0.0, 2.5, 5.0$, which almost match. It was already pointed out in [45, 49–52, 58–60] that the situation suddenly becomes weird in the process of the 2-solitons collision process. Apparently, the nonlinearity in the equation has a detrimental effect on how the solutions evolve. The sickness can be readily identified in the conservation laws, which, as we shown, are supported by the equation itself. In Fig.2, we illustrate the time dependency of the conserved quantity I_2 (6) of the 1-soliton and the 2-soliton configurations using the Runge-Kutta method with some selections of mesh points, such as $N_x = 150, 200, 250, 300, 350$ and $N_y = 200$. The behaviors in the 1-soliton solution are nearly

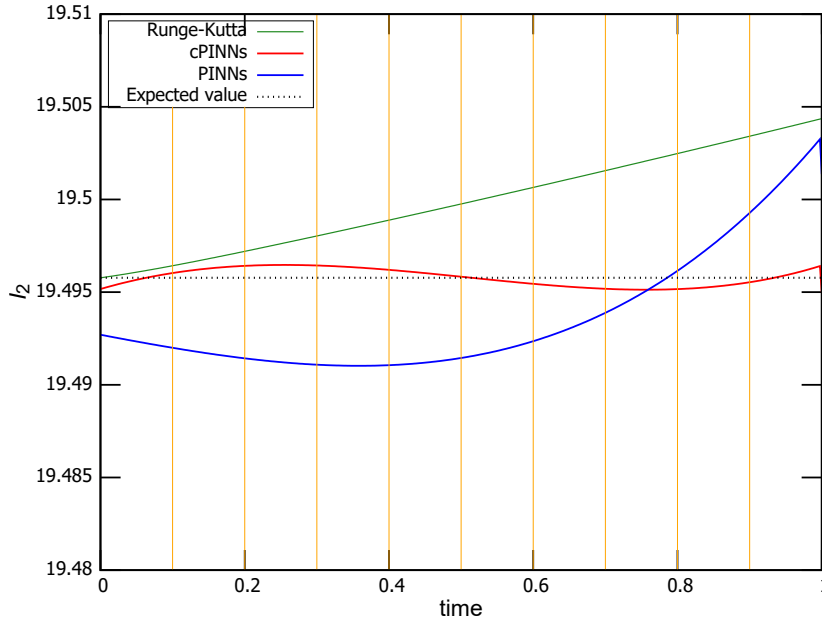


FIG. 4. The conserved quantity I_2 with $0 \leq t \leq 1$ of the configuration of the onset collision with $c = 1.0, 0.25$ of the Runge-Kutta, PINNs and cPINNs solutions.

flat within the numerical uncertainty and seem to converge to a constant value as the mesh points increase. It is natural to conclude that the 1-soliton solution of the equation exists in the limit of the infinite number of mesh points. However, we do not have such a solution for the 2-soliton as they exhibit both a modest, rapid fluctuation and a considerable divergence. The latter is more crucial since it subtly demonstrates that the 2-soliton configuration is not the solution to the equation, whereas the former might represent some chaotic feature of the system. Not only the I_2 , the other conserved quantities also exhibit similar behavior. Although some sophisticated numerical techniques such like the implicit method might improve the conservation, one cannot resolve the significant discrepancy seen in Fig.2. Consequently, we must draw the conclusion that the numerous collision process configurations of the several quasi-integrable equations found in earlier research [45] violated the equations' conservation nature. Further, the conserved quantities ought to be broken for the other multi-soliton configurations. The 2-soliton configuration is therefore considered as the DIFC, as we introduced the notion in the introduction. cPINNs, i.e., PINNs with keeping the conservation quantity enables us to seriously consider about the solutions that keep the conserved quantity.

Therefore, it is worthwhile to apply cPINNs to the collision process, as this approach surely yields the novel solution. We show the convergence property of PINNs and cPINNs of the solutions

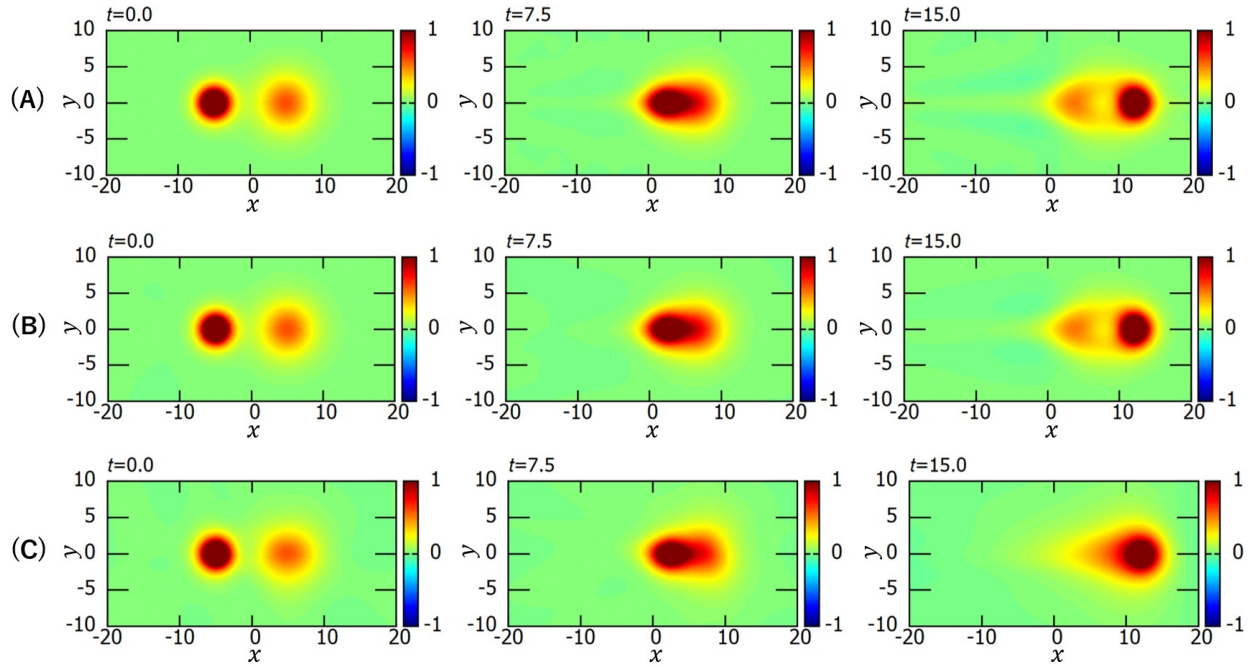


FIG. 5. The onset collision of the solutions with $c = 1.0$ and 0.25 of (A) the exact numerical analysis, (B) the PINNs, and (C) the cPINNs for the time $t = 0.0, 7.5, 15.0$.

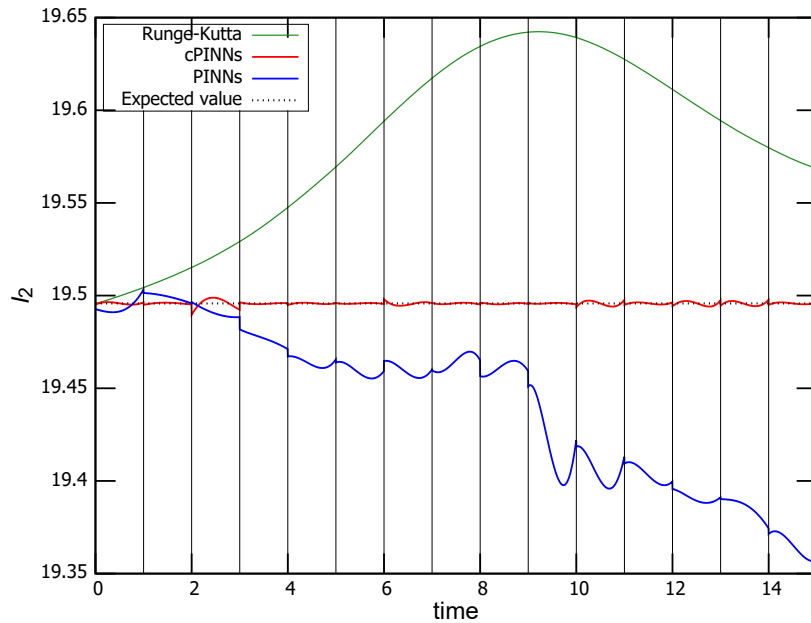


FIG. 6. The conserved quantity I_2 of the configurations of the onset collision with $c = 1, 0.25$ for longer time scale $0 \leq t \leq 15$ of Runge-Kutta, PINNs and cPINNs. For the PINNs, the cPINNs, we employ the analysis with the short time segments $[(s-1)\Delta t, s\Delta t]$, $s = 1, \dots, 15$; $\Delta t = 1.0$.

at the first time period $[T_0 = 0, T_0 + \Delta t]$. Fig.3 plots the MSEs of PINNs and cPINNs versus the iteration number. As we told, the convergence is attained for $|\nabla MSE| < \varepsilon$. Though the convergence of MSE_c is superior in cPINNs as anticipated, the total MES is much better in PINNs. It may seem strange because if the MSE had more conditions, the networks would provide a decent estimate of the actual solutions. The estimation of the conserved quantity I_2 using three distinct approaches might be used to explain the genesis of the unusual behavior (see Fig.4). The result indicates that there is never an exact conserved quantity in the solution, not just in the Runge-Kutta method. The solution of the collision process genuinely out of the submanifold of the conservative solution.

It is well known that some inelastic properties emerge when the heights of solitons are significantly different, in a collision process the taller soliton gains more height while the shorter one tends to wane with the radiation [45]. Fig.5 plots the collision of the 2-solitons of the velocity $c = 1.0$ and 0.25 . There is a slight difference between the numerical analysis and the PINNs, with the PINNs exhibiting a slight slowing (that is, a subtle dissipation) of the solitons. Ref.[45] also mentioned a further unusual behavior of the collision process. In case of the offset collision (the collision with finite impact parameter), the smaller soliton is almost diminished after the impact. Fig.6 plots the value of the conserved quantity I_2 for longer time scale. It is verified that cPINNs are efficient in identifying the solution that satisfies the conservation law. We show our analysis in Fig.7, where the discrepancy between the numerical analysis and the PINNs is more obvious. In Fig.8, we show the conserved quantity I_2 in the offset collision.

B. The successful inverse analysis

We define $\tilde{\mathcal{N}}$ for the inverse analysis for the ZK equation, using two unknown constants λ_0, λ_1

$$\tilde{\mathcal{N}}_{\text{ZK}}(u, u_x, u_{xxx}, u_{xyy}; \lambda_0, \lambda_1) := \lambda_0 u u_x + \lambda_1 (\nabla^2 u)_x. \quad (22)$$

We investigate the inverse analysis of PINNs for finding the parameter values (λ_0, λ_1) in terms of the training data derived from the numerical analysis, PINNs and cPINNs. In Table I, we present our result of the inverse analysis for the 1-soliton data. One can see that all the coefficients of the equation are quite well-reproduced in the analysis.

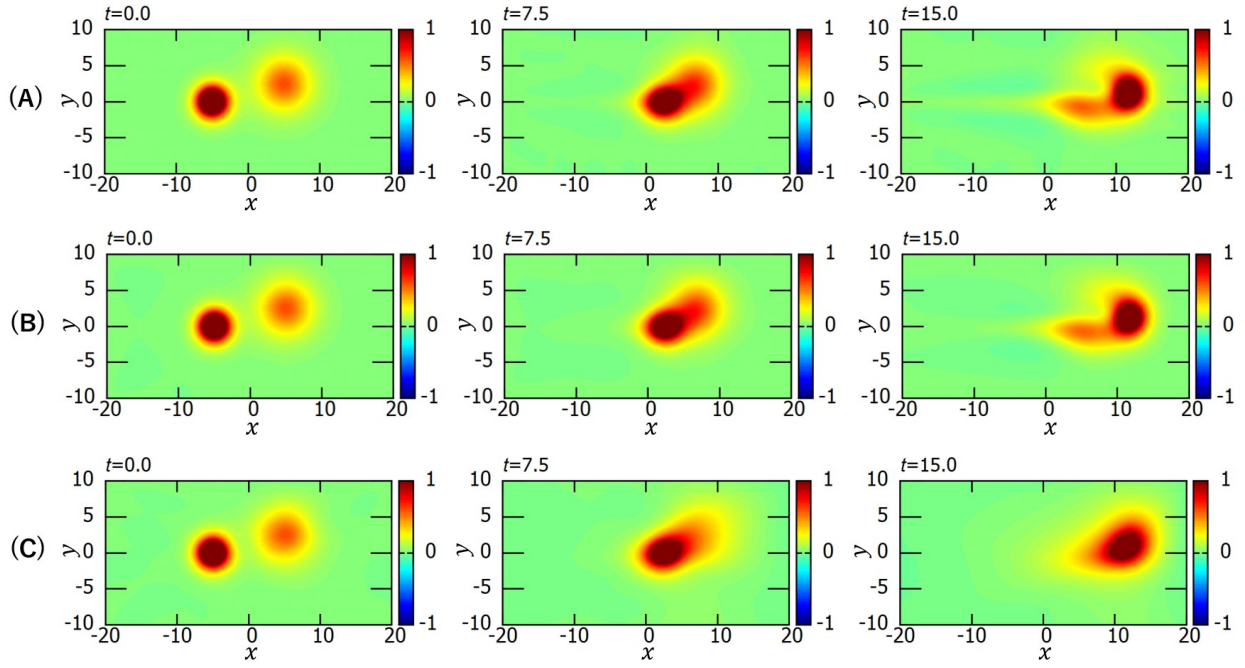


FIG. 7. The offset collision of the solutions with $c = 1.0$ and 0.25 of (A) the exact numerical analysis, (B) the PINNs, and (C) the cPINNs for the time $t = 0.0, 7.5, 15.0$.

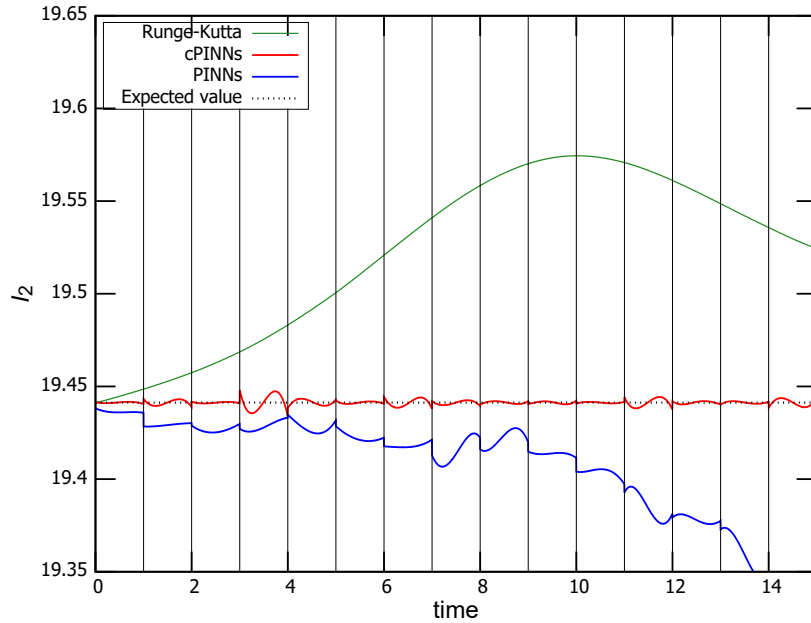


FIG. 8. The conserved quantity I_2 of the configurations of the offset collision (Fig.7) with $c = 1.0, 0.25$ for longer time scale $0 \leq t \leq 15$ of Runge-Kutta, PINNs and cPINNs.

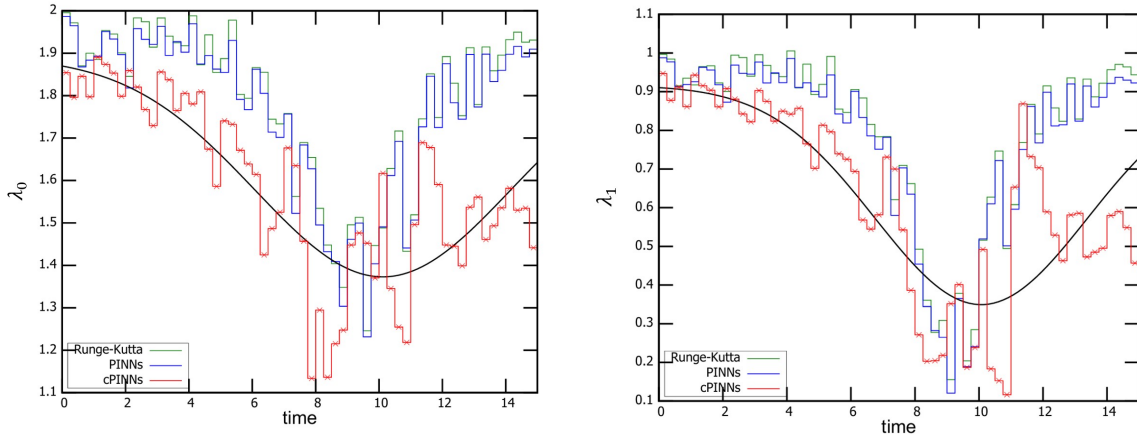


FIG. 9. The inverse analysis of the PINNs. The data is the onset collision with $c = 1.0$ and 0.25 of the exact numerical analysis, the PINNs, and the cPINNs for corresponding to Fig. 5(A),(B),(C). The inverse analysis is realized by the random sampling of the 50000th data points. We also add a solid line plot of an exponential fitting function of the cPINNs result defined by Eq.(24).

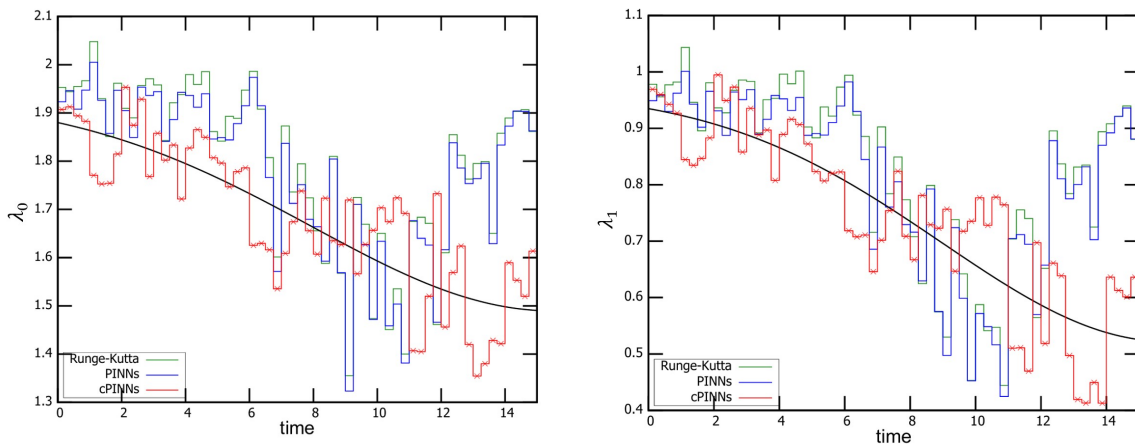


FIG. 10. The inverse analysis of the PINNs. The data is the offset collision with $c = 1.0$ and 0.25 of the exact numerical analysis, the PINNs, and the cPINNs for corresponding to Fig.7(A),(B),(C). The inverse analysis is realized by the random sampling of the 50000th data points. We also add a solid line plot of an exponential fitting function of the cPINNs result defined by Eq.(25).

TABLE I. *The successful* parameterization of the single-soliton solution

	PDE	$MSE (\times 10^{-6})$
correct	$u_t + 2uu_x + (\nabla^2 u)_x = 0$	—
exact	$u_t + 2.046uu_x + 1.0048 (\nabla^2 u)_x = 0$	4.4
PINNs	$u_t + 2.011uu_x + 1.0033 (\nabla^2 u)_x = 0$	4.6
cPINNs	$u_t + 2.011uu_x + 1.0033 (\nabla^2 u)_x = 0$	4.6

C. The temporal coefficients analysis via inverse PINNs

Now, we study the inverse analysis (22) of the 2-soliton training data, the results are shown in Figs.5 and 7. Instead of the entire set of data for the inverse analysis, we employ the data of the short period of segment, allowing us to estimate the true value of the coefficients with each segment. Such prescription was repeatedly used with several types of formulation to overcome the issue of reducing the computation cost for training a larger network [22, 61, 62]. Fig.9 plots the results of the modulation of the coefficients λ_0, λ_1 as a function of the time t in the onset collision process using data from the Runge-Kutta method, PINNs, and cPINNs. We compute them for the time segments $dt = 0.25$. The coefficients depart from their initial values, indicating a special temporal effect that is explicitly not implemented in the equation. The noteworthy is that the coefficients exhibit significant modulations, i.e., reducing the values during the impact and eventually returning to their initial values. Since the data with cPINNs is similar with the integrable one due to the conservation nature, it is natural to expect that the change of the coefficients ought to be suppressed. The result is totally opposite, with the cPINNs showing the most noticeable change. In Fig.10, we plot the similar analysis in the offset collision case. Notable feature in the cPINNs is that, after the collision the coefficients do not return to their initial value (a process called as the mutation), suggesting that the equation decays into the different regime.

D. Considerations for the modulations coefficients effect

As we saw in the previous subsection, we have observed the non-trivial modulations or mutations of the coefficients in terms of the data which are the configurations of the equation with constant coefficients. We consider PINNs inverse analysis exposed this effect for first time. It seems to happen only in the quasi-integrable equations, i.e., not in the integrable equations such as KdVs and nonlinear Schrödinger eq.. For those cases, both the forward and the inverse analysis are perfectly coincide in sense of the parameter mutations. The natural interpretation is temporal emergence of an effective interaction during the impact of the collision. It is difficult to evaluate such an interaction that was not included explicitly in the original equation. Therefore, we would like to approach in a different point of view. One helpful way to distinguish between integrable and quasi-integrable equations is to look for their exact solutions. As is well-known the KdV equation possesses the infinite number of the exact solutions. However, to the best of our knowledge, there are no analytical multi-soliton solutions to the ZK equation. A natural question is raised: Are

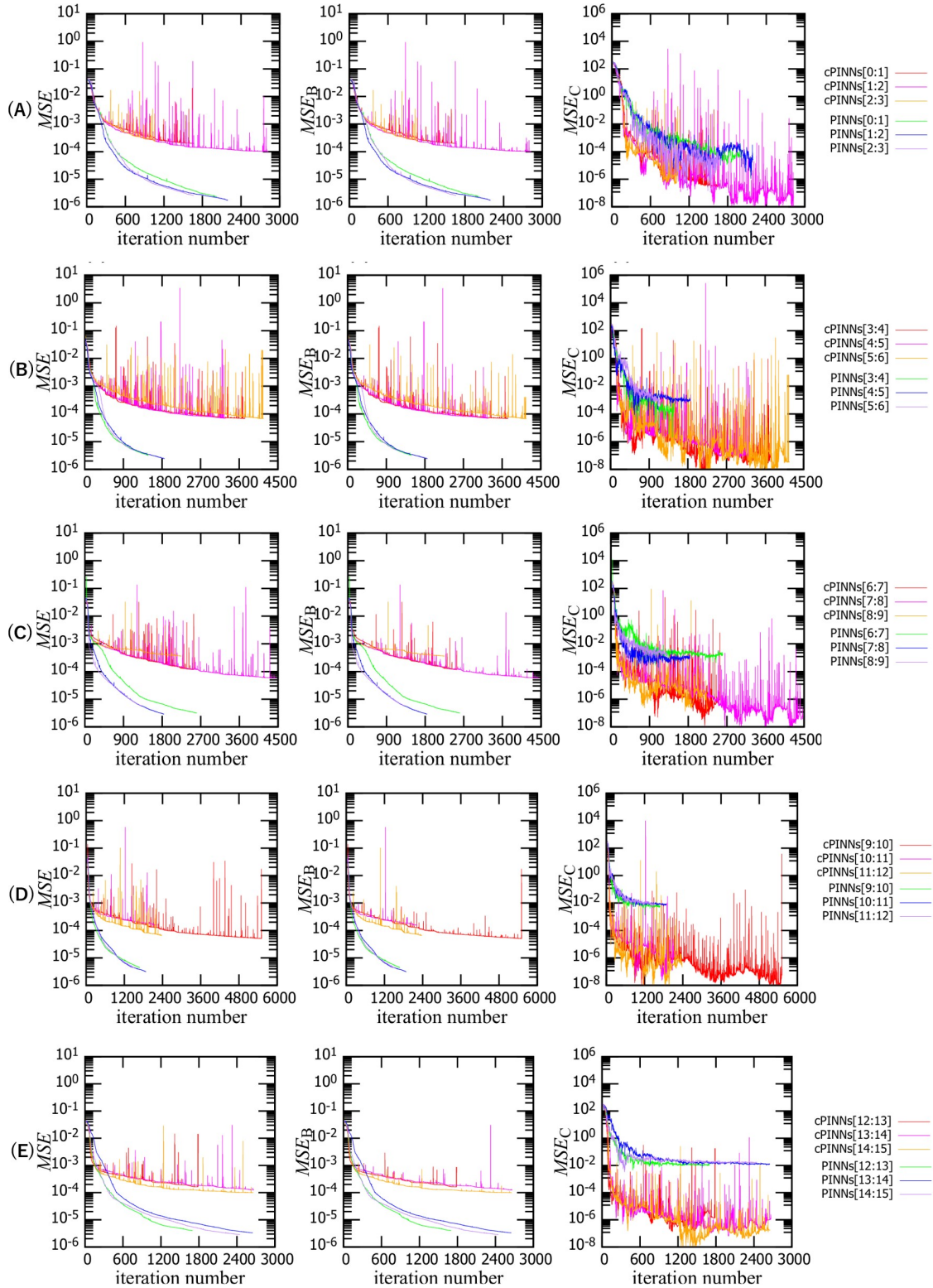


FIG. 11. The MSE of the onset collision of the solutions of $c = 1.0, 0.25$. For the visibility, we separate the data with fifth periods: (A)[0, 3],(B)[3, 6],(C)[6, 9],(D)[9, 12],(E)[12, 15]. The PINNs have cool colors, while the cPINNs have warm colors. We further divide the domains with the period $\Delta t = 1$ and plot by $[0, 1]$:red, $[1, 2]$:magenta, $[2, 3]$:orange for the cPINNs, for example. Each composed of the total MSE , the MSE_B , the MSE_C .

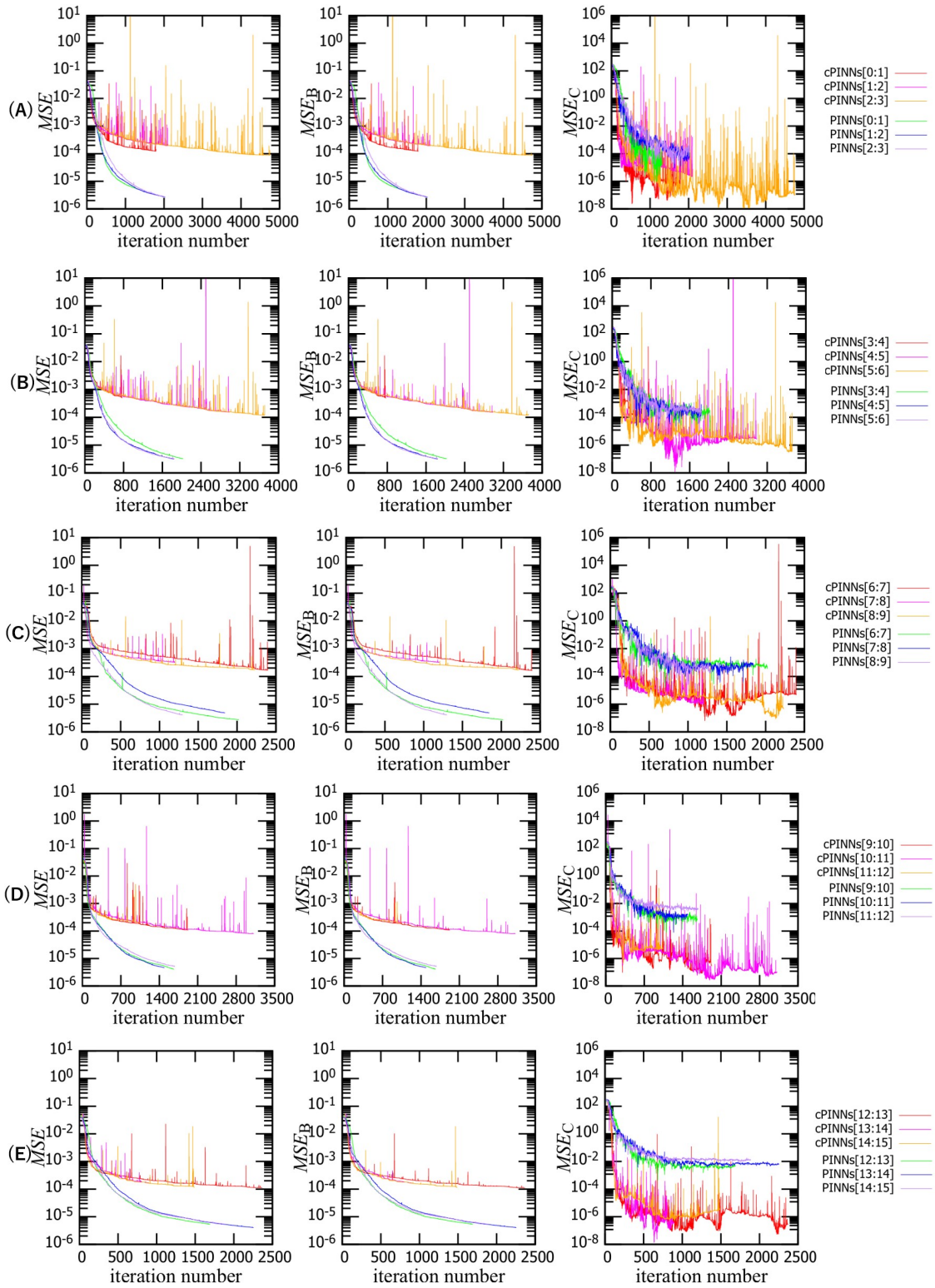


FIG. 12. The MSE of the offset collision of the solutions of $c = 1.0, 0.25$. For the visibility, we separate the data with five periods: (A)[0, 3],(B)[3, 6],(C)[6, 9],(D)[9, 12],(E)[12, 15]. The PINNs have cool colors, while the cPINNs have warm colors. We further divide the domains with the period $\Delta t = 1$ and plot [0, 1]:red, [1, 2]:purple, [2, 3]:orange, for example. Each composed of the total MSE , the MSE_B , the MSE_C .

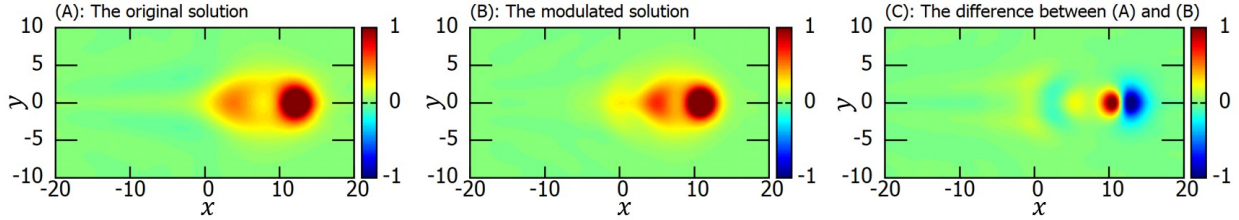


FIG. 13. The snapshot of the DIFC at $t = 15$ of the exact numerical analysis of the onset collision with $c = 1.0$ and 0.25 . (A) The exact numerical analysis for corresponding to Fig.5A, (B) the equation with the modulated coefficients (24), and (C) the the difference of (A) and (B).

the numerical 2-soliton “solutions” derived from PINNs or the Runge-Kutta method real solutions? The Runge-Kutta or other numerical method are based on the finite difference formalism. The solutions on the discrete space-time (or the wave number-angular frequency, anyway) are the good approximations of the genuine ones. However, because it might not have a continuous limit counterpart, the collision process is a DIFC. As we already stated, one of the distinguishing characteristics of PINNs is that they are based on the mesh-free algorithm. Therefore, the collision process does not directly solve the original equation, and, according to the inverse analysis the process is expressed using a modified equation. Concerning the forward PINNs or cPINNs, we have certain reservations. They are mesh-free but still we have the similar behaviour as the Runge-Kutta method. The hint is in the low convergence property of the result with PINNs. Fig.11 shows the MSE of PINNs and cPINNs of the collision process, corresponding to the solutions of Fig.5. The figures are composed of each fifth times periods for the visibility. The red, magenta, orange lines are result of cPINNs, and green, blue, cyan are the PINNs. The MSEs of PINNs are already an order of magnitude worse than the 1-soliton solutions. The cPINNs are even worse; the MSEs are roughly 10^{-4} , indicating that the original equation has no exact solution with sufficient low MESs. We may conclude that, in terms of PINN technology, we were successful in determining the correct equation for the collision of the quasi-integrable solitons. Fig.12 shows the MSEs of PINNs and cPINNs of the offset collision, corresponding to the solutions of Fig.7.

E. A 2-soliton in the equation with the modulated coefficients

As we have shown, the results of PINNs clearly imply that the equation may temporarily modulate, especially during the collision. Here, it is natural to re-examine the new equation with the modulated coefficients. The procedure is as follows: We start by examining an interpolating function for the temporal change of the coefficients in order to make the analysis tractable. Next, we

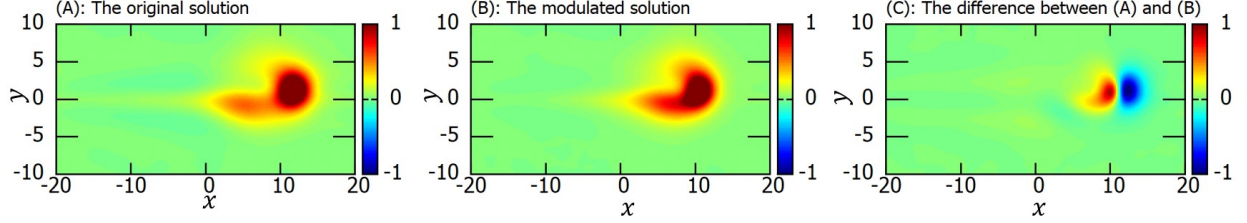


FIG. 14. The snapshot of the DIFC at $t = 15$ of the exact numerical analysis of the offset collision with $c = 1.0$ and 0.25 . (A) The exact numerical analysis for corresponding to Fig.5A, (B) the equation with the modulated coefficients (24), and (C) the the difference of (A) and (B).

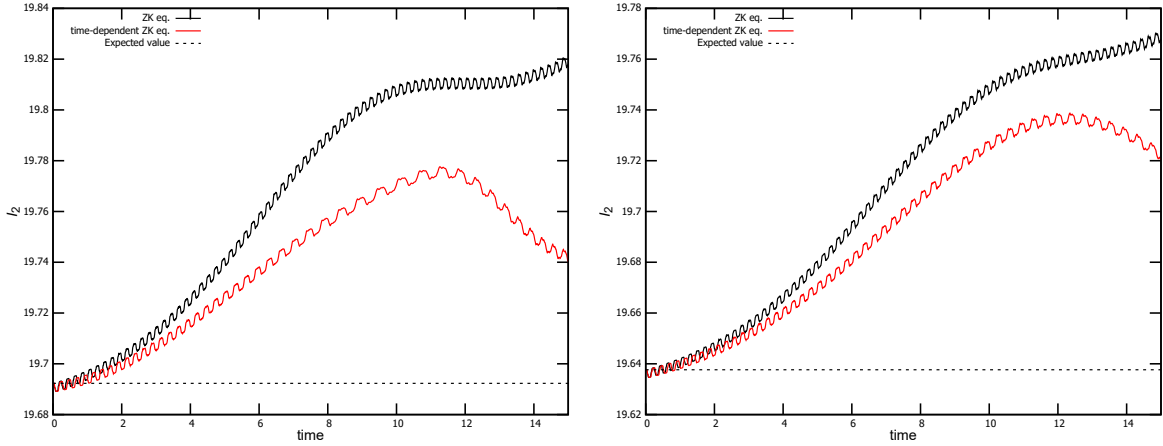


FIG. 15. The conserved quantity I_2 of the DIFC of the normal ZK equation and the time-dependent coefficients. Figure in the left plots the quantity I_2 for the onset collision of $c = 1.0$ and 0.25 in terms of the numerical analysis corresponding to Fig.5A. Also, the right is the offset collision corresponding to Fig.7A. The inverse analysis is realized by the random sampling of the 50000th data points.

solve the equation with that function in terms of the forward method (in this case, we use the Runge-Kutta method). Lastly, we analyze the conservation law I_2 with the obtained solution. For the form of the equation $\mathcal{N}_{ZK,mod} := \lambda_0 u u_x + \lambda_1 (\nabla^2 u)_x$, Here we employ a simple exponential fitting of the coefficients by

$$\lambda_i = a_i - \exp(b_i + c_i t + d_i t^2), \quad i = 0, 1 \quad (23)$$

with the eight fitting parameters a_i, b_i, c_i, d_i . We choose cPINN training data in this analysis because it shows a wider and greater shift in the coefficients, making the effect more noticeable than with PINNs or the Runge-Kutta method. For the change of the coefficient of the onset cPINNs

(Fig.9), the interpolating function can be fixed approximately as

$$\begin{aligned}\lambda_0 &= (1.892 \pm 0.069) - \exp [(-3.8 \pm 1.1) + (0.62 \pm 0.21)t + (-0.031 \pm 0.010)t^2] , \\ \lambda_1 &= (0.916 \pm 0.054) - \exp [(-5.1 \pm 1.3) + (0.91 \pm 0.25)t + (-0.046 \pm 0.013)t^2] ,\end{aligned}\quad (24)$$

which are also plotted as a solid line in Fig.9. We solve the equation with Eqs.(24) by the Runge-Kutta method. In Fig.13, we show the DIFC of the snapshot at $t = 15$ together with the original, non-modulated equations' one which was already presented in Fig.5. For the offset cPINNs, the interpolating function becomes

$$\begin{aligned}\lambda_0 &= (1.93 \pm 0.12) - \exp [(-2.9 \pm 1.7) + (0.27 \pm 0.24)t + (-0.0088 \pm 0.0098)t^2] , \\ \lambda_1 &= (0.965 \pm 0.076) - \exp [(-3.4 \pm 1.5) + (0.33 \pm 0.22)t + (-0.0106 \pm 0.0093)t^2] ,\end{aligned}\quad (25)$$

Again the behavior is put in Fig.10. The DIFC of the snapshot at $t = 15$ with the original one (Fig.7)is presented in Fig.14. The difference between the original and the mutated coefficients is obvious; the weaker solitons appear to be somewhat closer to the taller ones following the collision, whereas the taller solitons of the latter are ahead of the former. As a result, they tend to maintain their shape after impact. It suggests that the integrable nature recovers when the influences are lessened by the weaker coefficients. Therefore, we anticipate that there may be a 2-soliton DIFC to a novel variable coefficients equation [63–75].

Using the obtained DIFC, we evaluate the conservation quantity I_2 and plot the time dependency in Fig.15. There is still a large discrepancy, but the quantity tends to revert to the expected exact value as comparing the result using the original equation (Fig.2). If we wish to find the exact solution of the collision which possesses the perfect conservation laws, we recalculate the extra changing coefficients by computing the inverse PINNs once again using the data from Fig.13 or Fig.14, then repeat the procedure until the self-consistency is attained. By computing one extra step, we demonstrate how the iteration analysis proceeds. The interpolating function of the inverse PINNs result with the data from Fig.13 is defined as

$$\begin{aligned}\lambda_0 &= (1.839 \pm 0.019) - \exp [(-4.55 \pm 0.36) + (0.780 \pm 0.065)t + (-0.0360 \pm 0.0031)t^2] \\ \lambda_1 &= (0.887 \pm 0.011) - \exp [(-6.08 \pm 0.31) + (1.088 \pm 0.059)t + (-0.0515 \pm 0.0028)t^2]\end{aligned}\quad (26)$$

We show the modulation of the coefficients and the conservation quantity I_2 in Fig.16.

It appears that many iteration steps are required for the entire convergence, which obviously necessitates a large amount of computation time. In our typical analysis, the computations were carried out on four interconnected machines, each equipped with an Intel(R) UHD Graphics 730

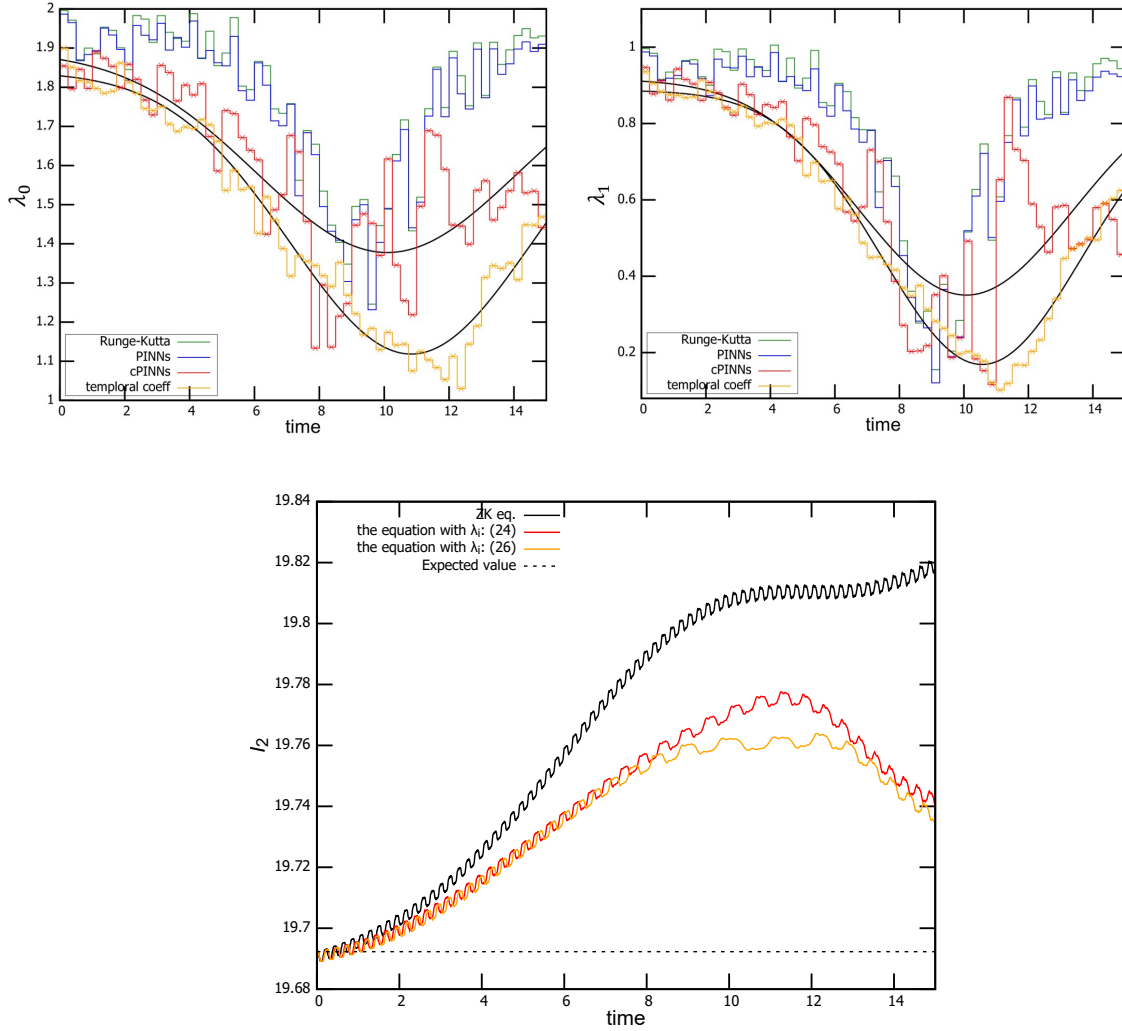


FIG. 16. The top two figures are the coefficients λ_0, λ_1 by the inverse analysis of the Runge-Kutta, PINNs and cPINNs where the data is DIFC of the onset collision with $c = 1.0$ and 0.25 and of the temporal coefficients. The inverse analysis is realized by the random sampling of the 50000th data points. We also add the solid line plots of an exponential fitting function of the cPINNs result defined by Eq.(24) and Eq.(26). The bottom figure is the resulting conserved quantity I_2 of the DIFC of the normal ZK equation and the time-dependent coefficients (24), (26).

GPU, 3.8 GB of memory, and an Intel Core i3-13100 CPU. The analysis takes roughly 75h per machine for one iteration step: 15h for the forward analysis of cPINNs and 60h for the inverse analysis. As a result, we have taken a very long time to achieve solution with sufficient convergence, necessitating significant technological advancements such as developing algorithms with more comprehensive capabilities and using more powerful machine.

IV. SUMMARY

In the present paper, we have investigated the PINNs for the analysis of the inelastic collision process of solitons in the quasi-integrable Zakharov-Kuznetsov equation. It is well-known that the process exhibits odd behavior, i.e., the taller soliton gains more height while the shorter one tends to wane with the radiation. We confirmed that all the conservation quantities are broken during the impact. Therefore, we introduced the conservative-PINNs and obtained the solution which was completely distinct from the known the Runge-Kutta or the normal PINNs solutions.

Employing the training data from the Runge-Kutta method, the PINNs and the cPINNs, we examined the inverse analysis for reconstructing the equation. We obtained the coefficients' mutation from constant values as we initially assumed, which seems crucial in the quasi-integrable systems. The natural interpretation of the effect is temporal emergence of an effective interaction during the impact of the collision. We determined the inverse PINNs using the data once more in order to investigate further mutation of the coefficients and get closer to the precise equation for the collision. Apparently, it requires numerous iteration steps then takes a lot of time to achieve solution conservation, requiring significant technological advancement. Of course, the best way is to construct the huge NN for the whole process, but it is out of scope of the present paper. We are able to state right now that we will present result of the aforementioned iterative method of a more simple, 1+1 dimensional case in our subesequent paper.

Acknowledgments The authors would like to thank Satoshi Horihata, Filip Blaschke, Sven Bjarke Gudnason, Luiz Agostinho Ferreira, Wojtek Zakrzewski and Paweł Klimas for many useful advices and comments. N.S. and K.S. would like to thank all the conference organizers of QTS12 and Prof. Āestmir Burdík for the hospitality and also many kind considerations. K.S. was supported by Tokyo University of Science. A.N., N.S. and K.T. were supported in part by JSPS KAKENHI Grant Number JP23K02794.

REFERENCES

-
- [1] Maziar Raissi, Alireza Yazdani, and George Em Karniadakis, “Hidden fluid mechanics: Learning velocity and pressure fields from flow visualizations,” *Science* **367**, 1026–1030 (2020),

- <https://www.science.org/doi/pdf/10.1126/science.aaw4741>.
- [2] Steven L. Brunton, Bernd R. Noack, and Petros Koumoutsakos, “Machine learning for fluid mechanics,” *Annual Review of Fluid Mechanics* **52**, 477–508 (2020).
 - [3] Teeratorn Kadeethum, Thomas M. Jorgensen, and Hamidreza M. Nick, “Physics-informed neural networks for solving nonlinear diffusivity and biot’s equations,” *PLOS ONE* **15**, 1–28 (2020).
 - [4] Mao Zhiping Wang Zhicheng Yin Minglang Karniadakis George Em Cai, Shengze, “Physics-informed neural networks (pinns) for fluid mechanics: a review,” *Acta Mechanica Sinica* (2021), 10.1007/s10409-021-01148-1.
 - [5] Kashinath K et al., “Physics-informed machine learning: case studies for weather and climate modeling,” *Phil.Trans.R.Soc.A* **379**, 20200093 (2021).
 - [6] Cai S. Li H. Karniadakis G.E Jin, X., “NSFnets (NavierStokes flow nets): Physics-informed neural networks for the incompressible Navier-Stokes equations,” *Journal of Computational Physics* **426**, 109951 (2021).
 - [7] Jiale Linghu, Weifeng Gao, Hao Dong, and Yufeng Nie, “Higher-order multi-scale physics-informed neural network (homs-pinn) method and its convergence analysis for solving elastic problems of authentic composite materials,” *Journal of Computational and Applied Mathematics* **456**, 116223 (2025).
 - [8] Ali Alhubail, Marwan Fahs, François Lehmann, and Hussein Hoteit, “Modeling fluid flow in heterogeneous porous media with physics-informed neural networks: Weighting strategies for the mixed pressure head-velocity formulation,” *Advances in Water Resources* **193**, 104797 (2024).
 - [9] Katayoun Eshkofti and Seyed Mahmoud Hosseini, “The modified physics-informed neural network (pinn) method for the thermoelastic wave propagation analysis based on the moore-gibson-thompson theory in porous materials,” *Composite Structures* **348**, 118485 (2024).
 - [10] Runze Sun, Hyogu Jeong, Jiachen Zhao, Yixing Gou, Emilie Sauret, Zirui Li, and Yuantong Gu, “A physics-informed neural network framework for multi-physics coupling microfluidic problems,” *Computers and Fluids* **284**, 106421 (2024).
 - [11] Rahul Rai and Chandan K. Sahu, “Driven by data or derived through physics? a review of hybrid physics guided machine learning techniques with cyber-physical system (cps) focus,” *IEEE Access* **8**, 71050–71073 (2020).
 - [12] Hao Wu, Feliks Nüske, Fabian Paul, Stefan Klus, Péter Koltai, and Frank Noé, “Variational Koopman models: Slow collective variables and molecular kinetics from short off-equilibrium simulations,” *The Journal of Chemical Physics* **146**, 154104 (2017), https://pubs.aip.org/aip/jcp/article-pdf/doi/10.1063/1.4979344/14899047/154104_1_online.pdf.
 - [13] Georgios Kissas, Yibo Yang, Eileen Hwuang, Walter R. Witschey, John A. Detre, and Paris Perdikaris, “Machine learning in cardiovascular flows modeling: Predicting arterial blood pressure from non-invasive 4d flow mri data using physics-informed neural networks,” *Computer Methods in Applied Mechanics and Engineering* **358**, 112623 (2020).
 - [14] Carlos Ruiz Herrera, Thomas Grandits, Gernot Plank, Paris Perdikaris, and Simone Sahli Costa-

- bal, Francisco and Pezzuto, “Physics-informed neural networks to learn cardiac fiber orientation from multiple electroanatomical maps,” *Engineering with Computers* **38**, 3957–3973 (2022).
- [15] Mohammadi Amirmohammad Pettigrew Roderic I. Jafari Roozbeh Sel, Kaan, “Physics-informed neural networks for modeling physiological time series for cuffless blood pressure estimation,” *npj Digital Medicine* **6**, 110 (2023).
- [16] Maziar Raissi, Paris Perdikaris, and George Karniadakis, “Physics informed deep learning (part i): Data-driven solutions of nonlinear partial differential equations,” (2017), 10.48550/arXiv.1711.10561.
- [17] Maziar Raissi, Paris Perdikaris, and George Karniadakis, “Physics informed deep learning (part ii): Data-driven discovery of nonlinear partial differential equations,” (2017), 10.48550/arXiv.1711.10566.
- [18] M. Raissi, P. Perdikaris, and G.E. Karniadakis, “Physics-informed neural networks: A deep learning framework for solving forward and inverse problems involving nonlinear partial differential equations,” *Journal of Computational Physics* **378**, 686–707 (2019).
- [19] Zhiwei Fang and Justin Zhan, “A physics-informed neural network framework for pdes on 3d surfaces: Time independent problems,” *IEEE Access* **8**, 26328–26335 (2020).
- [20] Francisco Sahli Costabal, Simone Pezzuto, and Paris Perdikaris, “Delta-pinns: Physics-informed neural networks on complex geometries,” *Engineering Applications of Artificial Intelligence* **127**, 107324 (2024).
- [21] Wenyuan Wu, Siyuan Duan, Yuan Sun, Yang Yu, Dong Liu, and Dezhong Peng, “Deep fuzzy physics-informed neural networks for forward and inverse pde problems,” *Neural Networks* **181**, 106750 (2025).
- [22] Ameya D. Jagtap, Ehsan Kharazmi, and George Em Karniadakis, “Conservative physics-informed neural networks on discrete domains for conservation laws: Applications to forward and inverse problems,” *Computer Methods in Applied Mechanics and Engineering* **365**, 113028 (2020).
- [23] Siddhartha Mishra and Roberto Molinaro, “Physics informed neural networks for simulating radiative transfer,” *Journal of Quantitative Spectroscopy and Radiative Transfer* **270**, 107705 (2021).
- [24] Xingzhuo Chen, David J. Jeffery, Ming Zhong, Levi D. McClenny, Ulisses M. Braga-Neto, and Lifan Wang, “Using physics informed neural networks for supernova radiative transfer simulation,” (2022).
- [25] Yu Yang, Helin Gong, Shiquan Zhang, Qihong Yang, Zhang Chen, Qiaolin He, and Qing Li, “A data-enabled physics-informed neural network with comprehensive numerical study on solving neutron diffusion eigenvalue problems,” *Annals of Nuclear Energy* **183**, 109656 (2023).
- [26] Alexandr Sedykh, Maninadh Podapaka, Asel Sagingalieva, Karan Pinto, Markus Pflitsch, and Alexey Melnikov, “Hybrid quantum physics-informed neural networks for simulating computational fluid dynamics in complex shapes,” *Machine Learning: Science and Technology* **5**, 025045 (2024).
- [27] Shuning Lin and Yong Chen, “A two-stage physics-informed neural network method based on conserved quantities and applications in localized wave solutions,” *Journal of Computational Physics* **457**, 111053 (2022).
- [28] Yin Fang, Gang-Zhou Wu, Nikolay A. Kudryashov, Yue-Yue Wang, and Chao-Qing Dai, “Data-driven soliton solutions and model parameters of nonlinear wave models via the conservation-law constrained

- neural network method,” *Chaos, Solitons and Fractals* **158**, 112118 (2022).
- [29] Gang-Zhou Wu, Yin Fang, Nikolay A. Kudryashov, Yue-Yue Wang, and Chao-Qing Dai, “Prediction of optical solitons using an improved physics-informed neural network method with the conservation law constraint,” *Chaos, Solitons and Fractals* **159**, 112143 (2022).
- [30] Elsa Cardoso-Bihlo and Alex Bihlo, “Exactly conservative physics-informed neural networks and deep operator networks for dynamical systems,” *Neural Networks* **181**, 106826 (2025).
- [31] A. Nakamura, N. Obuse, N. Sawado, K. Shimasaki, Y. Shimazaki, Y. Suzuki, and K. Toda, “Discovery of Quasi-Integrable Equations from traveling-wave data using the Physics-Informed Neural Networks,” (2024), arXiv:2410.19014 [physics.flu-dyn].
- [32] Jun Li and Yong Chen, “A deep learning method for solving third-order nonlinear evolution equations,” *Communications in Theoretical Physics* **72**, 115003 (2020).
- [33] J.C.Pu and Y.Chen, “Lax pairs informed neural networks solving integrable systems,” *J. Comput. Phys.* **510**, 113090 (2024).
- [34] Zhou Huijuan, “Parallel Physics-Informed Neural Networks Method with Regularization Strategies for the Forward-Inverse Problems of the Variable Coefficient Modified KdV Equation,” *J. Syst. Sci. Complex.* **37**, 511–544 (2024).
- [35] Shuning Lin and Yong Chen, “Physics-informed neural network methods based on miura transformations and discovery of new localized wave solutions,” *Physica D: Nonlinear Phenomena* **445**, 133629 (2023).
- [36] Zijian Zhou and Zhenya Yan, “Solving forward and inverse problems of the logarithmic nonlinear schrödinger equation with pt-symmetric harmonic potential via deep learning,” *Physics Letters A* **387**, 127010 (2021).
- [37] Juncai Pu, Jun Li, and Yong and Chen, “Solving localized wave solutions of the derivative nonlinear schrödinger equation using an improved pinn method,” *Nonlinear Dynamics* **105**, 1723–1739 (2021).
- [38] Qiongni Zhang, Changxin Qiu, Jiangyong Hou, and Wenjing Yan, “Advanced physics-informed neural networks for numerical approximation of the coupled schrödinger–kdv equation,” *Communications in Nonlinear Science and Numerical Simulation* **138**, 108229 (2024).
- [39] Z.W.Miao and Y.Chen, “Physics-informed neural networks method in high-dimensional integrable systems,” *Mod.Phys.Lett.B.* **36(1)**, 2150531 (2022).
- [40] Zijian Zhou, Li Wang, and Zhenya Yan, “Deep neural networks learning forward and inverse problems of two-dimensional nonlinear wave equations with rational solitons,” *Computers and Mathematics with Applications* **151**, 164–171 (2023).
- [41] Li Wang, Zijian Zhou, and Zhenya Yan, “Data-driven vortex solitons and parameter discovery of 2d generalized nonlinear schrödinger equations with a pt-symmetric optical lattice,” *Computers and Mathematics with Applications* **140**, 17–23 (2023).
- [42] UjjwalMishra Siddhartha Bai, GenmingKoley and Roberto Molinaro, “Physics informed neural networks (pinns) for approximating nonlinear dispersive pdes,” *Journal of Computational Mathematics*

- 39**, 816–847 (2021).
- [43] Z.Y. Yan Z.J. Zhou, L. Wang, “Deep neural networks learning forward and inverse problems of two-dimensional nonlinear wave equations with rational solitons,” *Comput. Math. Appl.* **151**, 164–171 (2023).
- [44] V. Zakharov and E A. Kuznetsov, “Three-dimensional solitons,” *Soviet Physics JETP* **29**, 594–597 (1974).
- [45] Hiroshi Iwasaki, Sadayoshi Toh, and Takuji Kawahara, “Cylindrical quasi-solitons of the Zakharov-Kuznetsov equation,” *Physica D: Nonlinear Phenomena* **43**, 293–303 (1990).
- [46] V. I. Petviashvili and V. V. Yan’kov, “Bilayer vortices in rotating stratified fluid,” *Dokl. Akad. Nauk SSSR* **267**, 825–828 (1982).
- [47] Christian Klein, Svetlana Roudenko, and Nikola Stoilov, “Numerical study of Zakhavor-Kuznetsov equations in two dimensions,” *Journal of Nonlinear Science* **31**, 1–28 (2021).
- [48] Yukito Koike, Atsushi Nakamura, Akihiro Nishie, Kiori Obuse, Nobuyuki Sawado, Yamato Suda, and Kouichi Toda, “Mock-integrability and stable solitary vortices,” *Chaos Solitons and Fractals: the interdisciplinary journal of Nonlinear Science and Nonequilibrium and Complex Phenomena* **165**, 112782 (2022), arXiv:2204.01985 [math-ph].
- [49] Kh.O. Abdulloev, I.L. Bogolubsky, and V.G. Makhankov, “One more example of inelastic soliton interaction,” *Physics Letters A* **56**, 427–428 (1976).
- [50] J. Courtenay Lewis and J.A. Tjon, “Resonant production of solitons in the rlw equation,” *Physics Letters A* **73**, 275–279 (1979).
- [51] F. ter Braak, L. A. Ferreira, and W. J. Zakrzewski, “Quasi-integrability of deformations of the KdV equation,” *Nucl. Phys. B* **939**, 49–94 (2019), arXiv:1710.00918 [hep-th].
- [52] Takuji Kawahara, Keisuke Araki, and Sadayoshi Toh, “Interactions of two-dimensionally localized pulses of the regularized-long-wave equation,” *Physica D: Nonlinear Phenomena* **59**, 79–89 (1992).
- [53] Thomas Brooke Benjamin, J. L. Bona, and J. J. Mahony, “Model equations for long waves in nonlinear dispersive systems,” *Philosophical Transactions of the Royal Society of London. Series A, Mathematical and Physical Sciences* **272**, 47–78 (1972).
- [54] E.A. Kuznetsov, A.M. Rubenchik, and V.E. Zakharov, “Soliton stability in plasmas and hydrodynamics,” *Physics Reports* **142**, 103–165 (1986).
- [55] Dong C. Liu and Jorge Nocedal, “On the limited memory bfgs method for large scale optimization,” *Mathematical Programming* **45**, 503–528 (1989).
- [56] Alex Bihlo and Roman O. Popovych, “Physics-informed neural networks for the shallow-water equations on the sphere,” *Journal of Computational Physics* **456**, 111024 (2022).
- [57] Aditi S. Krishnapriyan, Amir Gholami, Shandian Zhe, Robert M. Kirby, and Michael W. Mahoney, “Characterizing possible failure modes in physics-informed neural networks,” *Proceedings of the 35th International Conference on Neural Information Processing Systems, NIPS ’21* (2024).
- [58] Katuhiko Goda and Yoshinari Fukui, “Numerical studies of the regularized long wave equation,” *Journal*

- of the Physical Society of Japan **48**, 623–630 (1980), <https://doi.org/10.1143/JPSJ.48.623>.
- [59] Mitsuhiro Makino, Tetsuo Kamimura, and Tosiya Taniuti, “Dynamics of two-dimensional solitary vortices in a low- β plasma with convective motion,” *Journal of the Physical Society of Japan* **50**, 980–989 (1981), <https://doi.org/10.1143/JPSJ.50.980>.
- [60] L. A. Ferreira, G. Luchini, and Wojtek J. Zakrzewski, “The concept of quasi-integrability,” *AIP Conf. Proc.* **1562**, 43–49 (2013), arXiv:1307.7722 [hep-th].
- [61] Ameya D. Jagtap and George Em Karniadakis, “Extended physics-informed neural networks (xpinns): A generalized space-time domain decomposition based deep learning framework for nonlinear partial differential equations,” *Communications in Computational Physics* **28**, 2002–2041 (2020).
- [62] Hee Jun Yang and Hyea Hyun Kim, “Iterative algorithms for partitioned neural network approximation to partial differential equations,” *Computers and Mathematics with Applications* **170**, 237–259 (2024).
- [63] F. Calogero and Ao Degasperis, “Exact solution via the spectral transform of a generalization with linearly x -dependent coefficients of the modified korteweg-de-vries equation,” *Lett. Nuovo Cim* **22**, 270–273 (1978).
- [64] T. Brugarino and P. Pantano, “The integration of burgers and korteweg-de vries equations with nonuniformities,” *Physics Letters A* **80**, 223–224 (1980).
- [65] Nalini Joshi, “Painlevé property of general variable-coefficient versions of the korteweg-de vries and non-linear schrödinger equations,” *Physics Letters A* **125**, 456–460 (1987).
- [66] Ladislav Hlavatý, “Painlevé analysis of nonautonomous evolution equations,” *Physics Letters A* **128**, 335–338 (1988).
- [67] Tommaso Brugarino and Antonio M. Greco, “Painlevé analysis and reducibility to the canonical form for the generalized kadomtsev–petviashvili equation,” *Journal of mathematical physics* **32**, 69–71 (1991).
- [68] Yi-Tian Gao and Bo Tian, “Variable-coefficient balancing-act algorithm extended to a variable-coefficient mkp model for the rotating fluids,” *International Journal of Modern Physics C* **12**, 1383–1389 (2001).
- [69] Tadashi Kobayashi and Kouichi Toda, “A generalized kdv-family with variable coefficients in $(2+1)$ dimensions,” *IEICE Transactions on Fundamentals of Electronics, Communications and Computer Sciences* **88**, 2548–2553 (2005).
- [70] Tadashi Kobayashi and Kouichi Toda, “The painlevé test and reducibility to the canonical forms for higher-dimensional soliton equations with variable-coefficients,” *SIGMA. Symmetry, Integrability and Geometry: Methods and Applications* **2**, 063 (2006).
- [71] Xin-Yi Gao, Yong-Jiang Guo, and Wen-Rui Shan, “Optical waves/modes in a multicomponent inhomogeneous optical fiber via a three-coupled variable-coefficient nonlinear schrödinger system,” *Applied Mathematics Letters* **120**, 107161 (2021).
- [72] Xin-yi Gao, Yong-jiang Guo, Wen-rui Shan, Tian-yu Zhou, Meng Wang, and Dan-yu Yang, “In the atmosphere and oceanic fluids: Scaling transformations, bilinear forms, bäcklund transformations and solitons for a generalized variable-coefficient korteweg-de vries-modified korteweg-de vries equation,”

- China Ocean Engineering **35**, 518 (2021).
- [73] Xin-Yi Gao, Yong-Jiang Guo, and Wen-Rui Shan, “Similarity reductions for a generalized (3+1)-dimensional variable-coefficient b-type kadomtsev-petviashvili equation in fluid dynamics,” Chinese Journal of Physics **77**, 2707–2712 (2022).
- [74] Xin-Yi Gao, Yong Guo, and Wen-Rui Shan, “In nonlinear optics, fluid mechanics, plasma physics or atmospheric science: symbolic computation on a generalized variable-coefficient korteweg-de vries equation,” Acta Mathematica Sinica, English Series (2022).
- [75] Xiao-Tian Gao and Bo Tian, “Water-wave studies on a (2+ 1)-dimensional generalized variable-coefficient boiti–leon–pempinelli system,” Applied Mathematics Letters **128**, 107858 (2022).